UNITED NATIONS UNIVERSITY
UNU-GTP
Geothermal Training Programme

Orkustofnun, Grensasvegur 9,
IS-108 Reykjavik, Iceland

Reports 2018
Number 11

INTERPRETATION OF THERMAL FLUID CHEMISTRY DATA FOR WAESANO GEOTHERMAL WATER, EAST NUSA TENGGARA, INDONESIA

Margiet Candrikawati
Directorate of Geothermal
Ministry of Energy and Mineral Resources
Jl. Pegangsaan Timur No. 1, Menteng
Central Jakarta
INDONESIA
margiet89candrikawati@gmail.com

ABSTRACT

Seventeen samples from the Waesano geothermal area, Indonesia, have been interpreted to study the chemical characteristics, determine the type and origin of the waters, and estimate the reservoir temperature. In this study, Cl-SO_4-CHO_3, Li-Cl-B, and Na-K-Mg ternary diagrams, stable isotope ratios, geothermometers, and mixing models have been used to evaluate the results of the analysis of the samples. The results show that most of the samples plot as mature waters in the Cl-SO_4-HCO_3 ternary diagram, the samples appear to be in a partial equilibrium with the rock and apparently, they are associated with volcanism. Some samples show a $\delta^{18}O$ isotope shift in a $\delta D - \delta^{18}O$ diagram, meaning there is water-rock interaction. One sample, APWS-01, plots with a large $\delta^{18}O$ shift.

The Waesano geothermal water shows several characteristics of deep reservoir water such as a near-neutral pH, high salinity, high chloride, boron-rich composition, and a large $\delta^{18}O$ isotopic shift of up to 5‰ from the meteoric water line in a $\delta D - \delta^{18}O$ diagram. The Na-K geothermometer results give temperatures of 124-252°C. The temperatures obtained from log (Q/K) are 125-200°C, similar to the average for the Na-K geothermometer which is then interpreted as the reservoir temperature. The Na-K-Mg ternary diagram suggests a temperature in the range 160-265°C. Two types of mixing models have been applied to evaluate the temperature of the hot water component in the geothermal reservoir, the chloride-enthalpy model and the silica-enthalpy model. Together they indicate a reservoir temperature of 140-213°C. Based on four methods that have been used, a temperature in the range 200±70°C has been obtained, suggesting that the Waesano geothermal system is a medium temperature system.

1. INTRODUCTION

The Waesano geothermal area is located around Sano Nggoang Lake, West Manggarai, Flores Island and East Nusa Tenggara as shown in Figure 1 (Hadi et al., 2003). Thermal activity is manifested by hot springs with gas bubbling and sulphur deposition. This field is one of the high-temperature fields in Flores Island.

FIGURE 1: The investigation area entered, the West Manggarai Regency, Flores Island (Hadi et al., 2003)

Up to now, more geothermal development has taken place in western Indonesia than eastern Indonesia. The Indonesian government is acting to develop geothermal energy in eastern Indonesia and several significant geothermal developments in eastern Indonesia such as MEMR (the Indonesian Ministry of Energy and Mineral Resources) have been granted. Flores Island is an island that will utilize geothermal energy by direct and indirect uses, assigned as a State- Owned Entrepreneurship, and drilling, supported by the government, has started.

Flores Island encompasses 17 geothermal fields with an estimated resource potential of 402 MW with three fields assigned to the State-Owned Entrepreneurship, one field developed by a private company called PT Sokoria Geothermal Indonesia, and two fields will be subjected to government drilling projects. Even though the island has significant geothermal resources, there is no geothermal power generated there yet. The main electrical power source in Flores Island is still a reliance on small hydroelectric and expensive diesel generation.

The Waesano geothermal area will become the first government drilling pilot project with a potential capacity of 45 MW. The aim of government drilling is to reduce the geothermal business risk during upstream development. The Indonesian government will take part in the cost of unsuccessful exploration drilling to increase the attractiveness to private developers to engage in geothermal development in Indonesia.

Geothermal exploration was started in the Waesano field in 1997 by the Volcanology Agency and included studies of heat loss and geological structures around the Waesano area. In 2004, the Geological Agency as a representative of the Indonesian government conducted a number of exploration surveys including geological studies, geophysical surveys, and geochemical sampling. In 2015 they conducted further investigations into the geology and geochemistry of the Sano Nggoang district, West Manggarai (Figure 1), and East Nusa Tenggara due to the emergence of new hot springs in the North Sano Nggoang district, around Sano Limbung Lake. A geothermal resource evaluation was completed in 2015 with a

potential estimation of 45 MW and in 2017 the Minister of Energy and Energy Resources designated Waesano as a Geothermal Working Area through decision number 4330 K/30/MEM/2017. The designated area measures 12,190 hectares.

Samples were collected by the Geological Agency in 2014 and Jacobs New Zealand Limited as a consultant for the World Bank in 2016, including hot spring water and cold water. Seventeen samples have been chosen for this study which focuses on the interpretation of thermal fluid chemistry data for the Waesano geothermal water (Figure 2).

FIGURE 2: The Waesano geothermal field and water sample locations (GoogleEarth)

The reservoir temperature was estimated with the aid of various geothermometer calculations. In this study, mixing models have been used in an effort to understand the physical processes which take place in the geothermal system and the interpretation of thermal fluid composition will give a better understanding of the origin of the fluid and the chemical processes that take place during ascent.

2. GEOLOGICAL STRUCTURE AND SURFACE MANIFESTATIONS

The tectonics of Indonesia are complex and unique due to its location at the junction of three tectonic plates, that is the Indian-Australia plate to the south, the Pacific Plate to the west, and the Eurasian Plate to the north. Indonesia is located between two continental plates, the Eurasian Plate and the Australian Plate (Sahul Shelf) and two oceanic plates, the Philippine Sea Plate and the Pacific Plate (Figure 3).

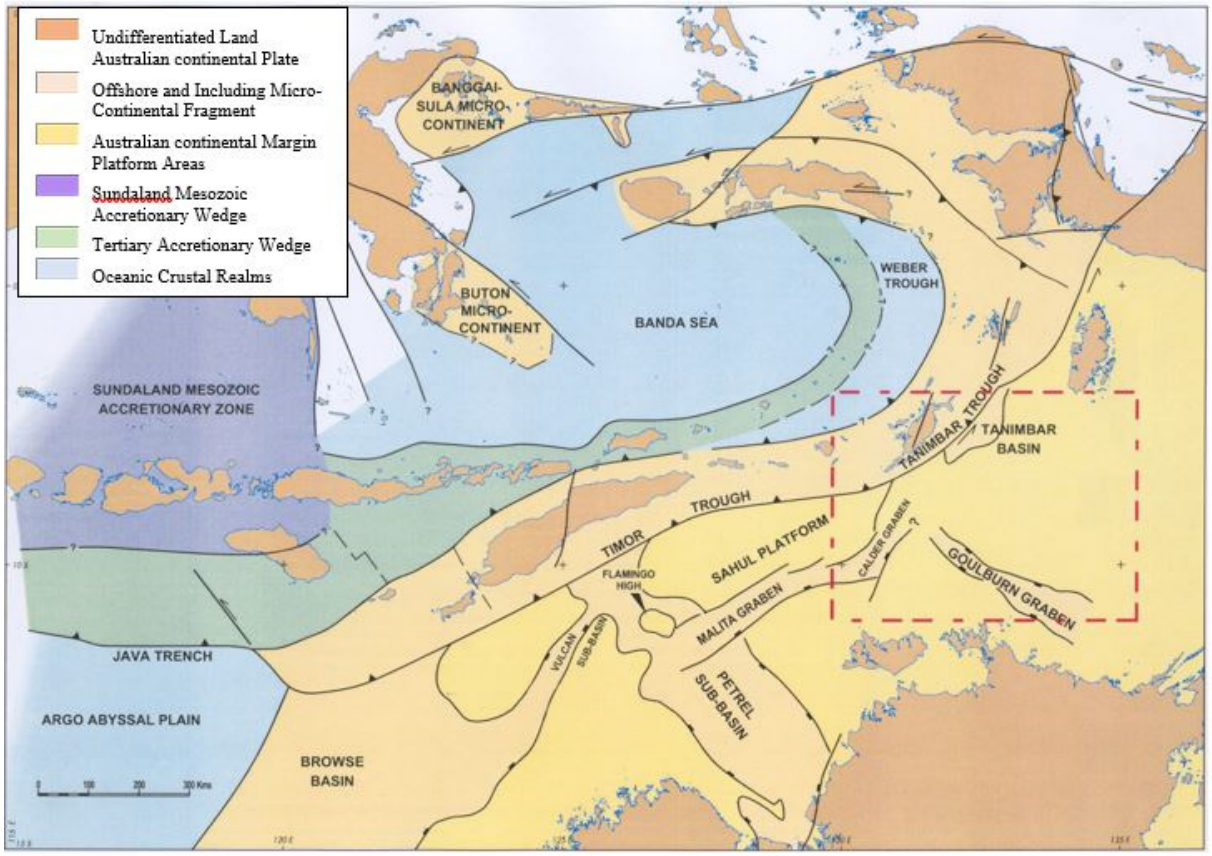

FIGURE 3: East Indonesia and northern Australia continental margin regional tectonic elements (Barber et al., 2003)

The geological structures of eastern Indonesia are more complex than those of western Indonesia due to the junction of the three tectonic plates, the Pacific plate, the Australian plate, and the Eurasian plate, composed of micro plates except the Nusa Tenggara, North Irian, East Irian and North Sulawesi areas. Eastern Indonesia is where the island arc system has formed.

The presence of geothermal energy in Indonesia is generally controlled by volcanic systems. The chain of active volcanoes has formed along the Sumatera, Java, Bali, and Nusa Tenggara islands. The volcanic system in Nusa Tenggara islands is a result of subduction of the Indian oceanic plate beneath the Eurasian continental plate since mid-Tertiary. Thus, the stratigraphy of Eastern Indonesia is generally older than that of the western part. The age ranges from Permian to Tertiary.

2.1 Geological structure

In Indonesia, there are four arcs: The Sunda arc in the west, Banda arc in east, Sangihe-North Sulawesi and Halmahera arc in the north (Nasution et al., 2002). Flores Island is a part of the Banda arc, together with Bali, Lombok, Sumbawa, Flores, Alor and Wetar. This arc sector is a continuation of the Sunda island arc tectonic zone which extends through the islands of Sumatera and Java in western Indonesia (Johnstone, 2005). Based on Indonesia's geothermal potential inventory of the Indonesian MEMR published in 2017, 26 geothermal prospects have been identified along the Banda arc islands, from Lombok in the west to Alor in the east, with four on Bali, two on Lombok, one on Sumbawa, 17 on Flores, one on Alor, and one on Wetar (Directorate of Geothermal, 2017). Due to the geothermal potential in Flores Island, MEMR designated Flores Island to be a geothermal island based on decision number 2268 K/30/MEM/2017. Recently five prospects in the Banda Arc and all prospects in Flores Island have entered the exploration stage.

Tectonic activity in Flores Island is controlled by volcanic systems. Tectonic activity is the influence of the subduction of the Indian oceanic plate beneath the Eurasian continental plate, which took place during mid-Tertiary. The volcanic activity has produced new cones and domes on Mount Ranakah and Mount Waesano (Figure 4). Hydrothermal activity is common in Tertiary rocks associated with volcanic systems where granodiorite has formed. Hydrothermal changes are seen in Tertiary volcanoes along fault zones.

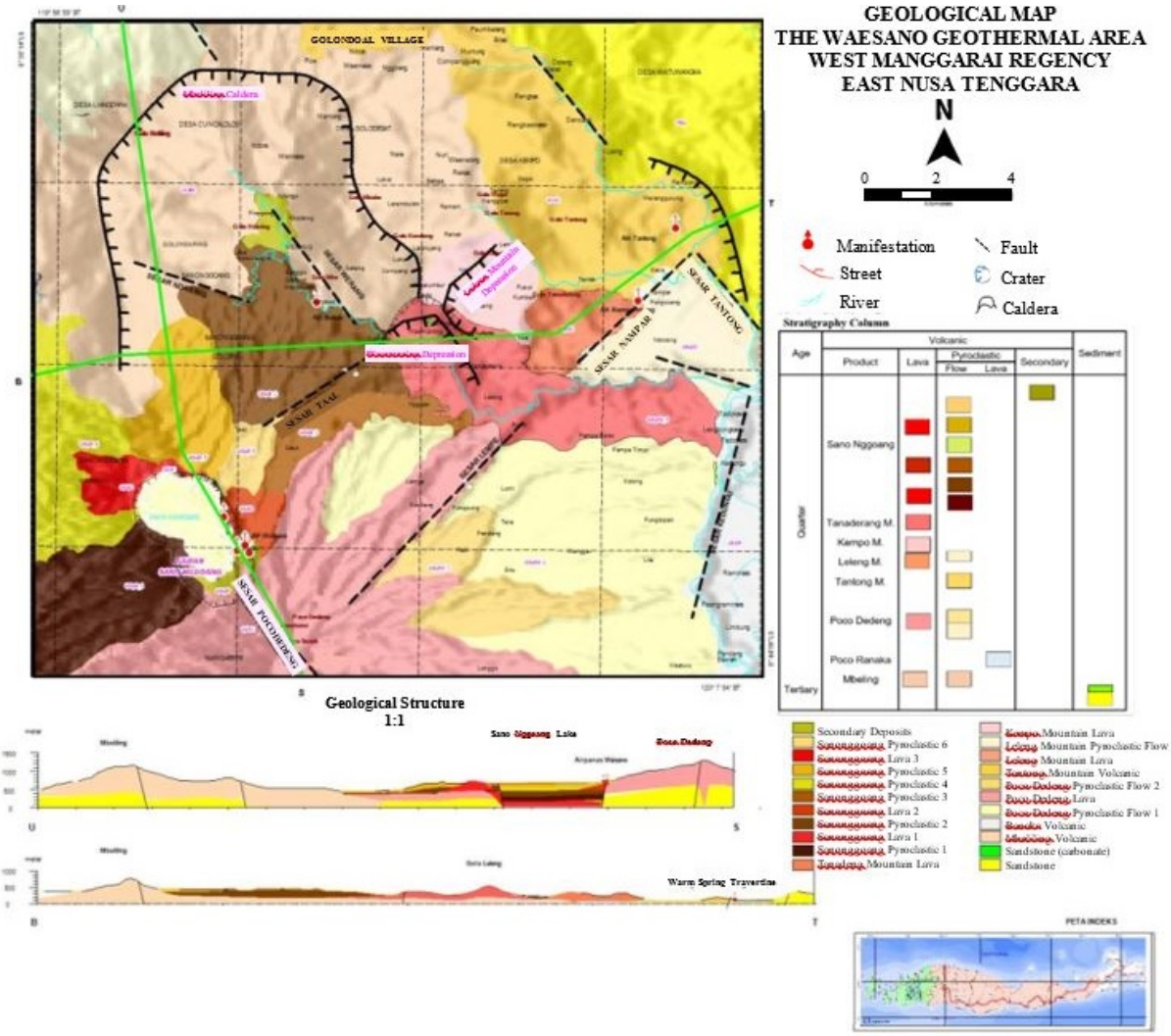

FIGURE 4: Geological structures in Waesano geothermal field (Hadi et al., 2003)

Geological structures divide faults as a result of volcanic activity, such as calderas, craters and the straightness of the fault. There are three geological structures in Werang – Wae Sano:

- The Nampar Mancing normal fault structure. This fault is marked as a triangular facet in mountain slopes/hills as a result of erosion, topographic alignments, and the emergence of hot springs/cold springs. This fault is directed ENE – WSW.
- The Wai Racang (Bobo) normal fault structure. This fault is marked with the emergence of hot springs/cold springs along the Wai Racang River. The hot water has mixed with cold water from the river.
- The Wae Sano (Sano Nggoang) caldera structure. This caldera is an elliptical lake at an elevation of 643 meters above sea level with a diameter of 3 km at the longest and 1 km at the shortest and a depth of around 30 meters and it is directed northwest – southeast.

2.2 Surface manifestations

Thermal activity in the Waesano geothermal area is centred on a crater lake called Lake Sano Nggoang and is marked by the appearance of geothermal manifestations along the edge of the lake such as rock alteration, fumaroles, sinter, hot springs, and warm springs. The highest temperature of 97°C is found at an elevation of above 640 m.

There are hot springs and warm springs surrounding the lake and the main area is on the eastern shore of Lake Sano Nggoang. Silica sinter is found in the hot springs, and the fluids are slightly acid and highly saline. The well WS-01, which is in this area, has heavy deposits of sulphur in the outflow. Hot water flows into the lake. A group of warm springs such as Nampar Mancing and Golo Lara appear in the north east part of Waesano and their temperature is around 30-50°C, pH 6-7 with a small flow, clear water, no smell, and saline. Sinter carbonate and sinter travertine are found in the warm springs and their geothermal characteristics are thus different from those of the Sano Nggoang manifestations. Carbonate sinter appears when the hot fluid flows to surface and dissolves large amounts of Ca. A group of cold water from the Lake Sano Nggoang outlet (WS-08), cold water from the Wae Sapo River (ADSA), cold water from Cunca Rami waterfall (ADCR), and cold water from the Pinggong River (ADPI). Their temperature is around 23-25°C, pH 7 except at the Lake Sano Nggoang outlet with pH 2.6. The cold waters have a small flow, clear water, no smell, and are not saline.

Hydrothermal alteration has taken place in Waesano due to the interaction of hot fluid at neutral/acid pH with the surrounding rock. Hydrothermal minerals identified in the Waesano field are dominated by haloysite, calcite, montmorillonite, kaolinite, pyrophillite, illite, paragonite, gypsum, diaspore, and jarosite. Considering that minerals associated with caprock indicate a low temperature and a neutral pH the presence of the minerals montmorillonite and haloysite suggests a temperature estimated around 150°C with a neutral pH and located in an argillic zone. The presence of pyrophillite, illite, kaolinite, dickite and alunite indicates an estimated temperature of <200°C with acid pH. The presence of gypsum indicates that there are reactions between sulphur and calcite and signs of the presence of sulphur sediment at the surface.

Waesano is regarded as a relatively old Quaternary volcano since no historic eruptions have been recorded. However, there are many features of the topography suggesting that the volcanism is not that old and certainly likely to be less than 1 Ma (Johnstone, 2005).

3. METHODOLOGY

3.1 Classification of thermal waters

3.1.1 Origin of geothermal waters

Isotope techniques are useful tools to investigate the origin of geothermal waters by determining the hydrogen and oxygen isotope ratios of water and steam from geothermal fields. Craig (1963) showed that geothermal fluids originate mainly in meteoric water.

The isotope ratios of $^{18}O/^{16}O$ and $^{2}H/^{1}H$ play an important role in geothermal water investigations. The $^{18}O/^{16}O$ ratio is an isotope tracer, and together with $^{2}H/^{1}H$ ratio it is a valuable indicator of mixing and vapour separation processes. Unlike $\delta^{18}O$, δD is hardly affected by exchange processes due to the low hydrogen content of rock compared to that of oxygen.

The $\delta^{18}O$ value for meteoric waters at any locality is therefore dependent upon latitude, altitude, and distance from the ocean (Nicholson, 1993). Samples from high latitudes and high elevation are lighter (more negative δ values). The values for δD and $\delta^{18}O$ in precipitation have been used to construct the world meteoric line with the following expression:

$$\delta D = 8(\delta^{18}O) + 10 \quad (1)$$

The δD is found to be constant and the same as that of the local meteoric waters of the area, while the $\delta^{18}O$ may show a characteristic enrichment which is known as oxygen isotope shift, that means that the $\delta^{18}O$ is higher (less negative) than that of the local meteoric water. The geothermal reservoir is formed from infiltration of meteoric waters with relatively low $\delta^{18}O$ at depth. In order to reach equilibrium corresponding to the temperature of the reservoir, there is a need to exchange oxygen with the surrounding rocks that are much richer in heavy isotopes. That makes the $\delta^{18}O$ values in geothermal waters often high as a result of isotope exchange between the water and the rock minerals which are richer in $\delta^{18}O$ at a high temperature.

The isotope exchange often takes place when the waters have moved. The degree of the isotope exchange depends on the proportions of the oxygen in the water and rocks, initial $\delta^{18}O$ value, the water-mineral fractionation factor, reaction time, and the surface contact area (Craig, 1963; Mainza, 2006).

3.1.2 Cl-SO_4-HCO_3 ternary diagram

This diagram is used for the classification of thermal water based on the concentration of the three major anions, Cl^-, SO_4^{2-}, and HCO_3^- which are plotted in a triangular diagram. The results give an initial indication for several typical groups of waters such as volcanic waters and steam-heated waters (SO_4^{2-}), peripheral waters (HCO_3^-), and mature waters (Cl^-). The Cl-SO_4-HCO_3 ternary diagram can be used to classify the geothermal waters as equilibrated, non-equilibrated, and mixed waters. Non-equilibrated water is not suitable for geothermometry (Giggenbach, 1988).

Chloride is a conservative ion in geothermal water and does not take part in reactions with the rocks due to the fact that once chloride has dissolved, it is usually not precipitated. CO_2 often enters the waters at low temperatures. The concentration of HCO_3 will increase with time and distance travelled underground (Giggenbach, 1988).

3.1.3 Cl-Li-B ternary diagram

The Cl-Li-B ternary diagram is used to trace the origin of thermal fluids. Lithium is used as a tracer for deep rock dissolution due to it being least affected by secondary processes of the alkali metals. The existence of lithium can be used as a reference for evaluating the possible origin of thermal waters based on the main conservative constituents of thermal waters, chloride and boron (Giggenbach, 1991).

At high temperatures, Cl occurs largely as HCl and B as H_3BO_3. Both components are volatile and easily mobilized by high temperature steam. At low temperatures, HCl is converted by the rock to the less volatile NaCl while B will remain in its volatile form to be carried in the vapour phase. The presence of B in thermal water probably reflects the degree of maturity of a geothermal system as B is not found in old hydrothermal systems, as due to its volatility B will disappear during an early heating stage. As B and Cl are the main conservative constituents, the Cl/B ratio is often used to indicate a common reservoir source for the waters.

3.1.4 Na-K-Mg ternary diagram

Giggenbach (1988) proposed the Na-K-Mg ternary diagram as a method to determine reservoir temperature and to classify waters into fully equilibrated, partially equilibrated and immature waters. The classification acts as a guide to which waters are most suitable for geothermometry. The fully equilibrated water is most useful for geothermometry, but the partially equilibrated waters are less reliable for geothermometers and immature water can be excluded as the geothermometers are based on equilibria during water-rock interaction. The area of partial equilibrium is less useful but can suggest mixing between equilibrated geothermal water and cold groundwater.

3.2 Geothermometers

3.2.1 Silica geothermometers

Silica geothermometers are based on experimentally determined and temperature dependent equilibria. Silica can be present in various forms in geothermal fields, such as quartz, cristobalite, chalcedony, or amorphous silica, that give rise to different geothermometers based on silica solubility of different silica species with respect to temperature and pressure.

Silica geothermometers with different forms of silica are simple up to about 250°C. The solubility temperature curve departs significantly from linearity after that, but reliable equations covering higher temperatures have been derived.

$$SiO_{2(qtz)} + 2H_2O = H_4SiO_4 \quad (2)$$

The quartz geothermometer is based on quartz solubility in which quartz will appear at temperatures above 120°C – 180°C. Several formulas have been proposed for the quartz geothermometer, given in Table 1.

TABLE 1: Equations for the quartz geothermometer from several experiments (Arnórsson, 2000)

Geothermometer	Equation (t in °C and S represents SiO_2 in mg/kg)	Source
Quartz – no steam loss	$\frac{1309}{5.19 - \log S} - 273.15$	Fournier (1977)
Quartz – maximum steam loss	$\frac{1522}{5.75 - logS} - 273.15$	Fournier (1977)
Quartz	$-42.2 + 0.28831S - 3.6686 \times 10^{-4}S^2 + 3.1665 \times 10^{-7}S^3 + 77.034logS$	Fournier and Potter (1982)
Quartz	$-55.3 + 0.3659S - 5.3954 \times 10^{-4}S^2 + 5.5132 \times 10^{-7}S^3 + 74.360logS$	Arnórsson et al. (1998)

The quartz geothermometer is usually the most reliable for reservoir temperatures above 150°C. Below that temperature, chalcedony is likely to control the dissolved silica concentration. The quartz geothermometer may be problematic for reservoir temperatures from 230 to 250°C due to quartz dissolving and precipitating very fast at temperatures above about 230°C (Fournier, 1973). In the temperature range 250-330°C, the silica geothermometer is the most useful when applied to waters produced from geothermal wells, where movement from the reservoir to the surface is rapid.

The chalcedony geothermometer is based on chalcedony solubility in which chalcedony will appear at temperatures of 100-120°C and lower. Chalcedony is a fine-grained variety of quartz, which is shown to be a mixture of quartz and moganite which, with time, will change to quartz (Gíslason, et al., 1997). Chalcedony is unstable in contact with water at temperatures above about 120°C due to the smallest sized crystals completely dissolving and larger sized crystals replacing them. Temperature, time, fluid composition and previous history (recrystallization of amorphous silica versus direct precipitation of quartz), all affect different crystalline forms of silica. In old geothermal systems where waters have been in contact with rock for a relatively long time, quartz as a well-crystallized form may control dissolved silica at temperatures below 100°C, and in young systems, chalcedony as a fine-grained quartz may control silica at temperatures up to 180°C.

Equations for the chalcedony geothermometer have been presented by Fournier (1977) and Arnórsson et al. (1983). These equations are applicable only for reservoir temperatures in the range 20-250°C, with silica concentration, SiO_2, in mg/kg:
Fournier (1977):

$$t(°C) = \frac{1032}{4.69 - logSiO_2} - 273.15 \quad (3)$$

and, Arnórsson, et al. (1983):

$$t(°C) = \frac{1112}{4.91 - logSiO_2} - 273.15 \quad (4)$$

3.2.2 Cation geothermometers

Cation geothermometers are based on the partitioning of alkalis between solid and liquid phases. Cation geothermometers include the Na/K geothermometer, the Na-K-Ca geothermometer, the Na-K-Ca-Mg geothermometer, and others like the Na-Li, K-Mg geothermometers.

Na-K geothermometer (Table 2). The Na/K ratios in geothermal waters are controlled by the equilibrium cation exchange reaction between the geothermal water and alkali feldspars. The equilibrium of cation exchange will affect the temperature. The reaction of Na^+ and K^+ exchange in a feldspar reaction is expressed as:

$$NaAlSi_3O_8 + K^+ = KAlSi_3O_8 + Na^+ \quad (5)$$

The equilibrium constant being:

$$K_{eq} = \frac{[KAlSi_3O_8][Na^+]}{[NaAlSi_3O_8][K^+]} \quad (6)$$

To simplify the equation, feldspar is assumed to be an almost pure solid, and assuming the activity of solid as ~1, the equation becomes:

$$K_{eq} = \frac{[Na^+]}{[K^+]} \quad (7)$$

TABLE 2: Equation for the Na-K geothermometer from several experiments (Arnórsson, 2000)

Geothermometer	Equation (t in °C)	Source
Na-K	$\frac{856}{0.857 + log(Na/K)} - 273.15$	Truesdell (1976)
Na-K	$\frac{1217}{1.438 + log\,(Na/K)} - 273.15$	Fournier (1979)
Na-K	$\frac{1390}{1.750 + log(Na/K)} - 273.15$	Giggenbach (1988)

There are many experimental results giving rise to Na-K geothermometers with various temperature functions. The results differ for different geothermometers chiefly due to the fact that experiments have been carried out with different minerals. This geothermometer is suitable for reservoir temperatures above 180°C and may give misleading results for low temperature water due to the equilibrium between feldspars an geothermal waters not being attained at low temperatures.

Na-K-Ca geothermometer. Fournier and Truesdell (1973) presented a geothermometer equation based on the exchange reaction of the cations Na^+, K^+, and Ca^{2+} with a mineral solid solution. This geothermometer is not suitable for waters with high concentrations of CO_2 or Ca. However, the Na-K-Ca geothermometer will work well if calcite was not deposited after the water left the reservoir. The main effect of the presence of calcite is the Na-K-Ca temperature becoming too high. The advantage of this geothermometer is to minimize the effects of disregarding the activity coefficient of solids. Another advantage is that it does not give high and misleading results for cold and slightly thermal, non-equilibrated waters (Arnórsson, 2000). This geothermometer assumes different formulae for temperatures above 100°C and below 100°C (Equation 8):

$$t\,(°C) = \frac{1647}{\log\,([Na^+]/[\,K^+]) \;\; + \;\beta \log(\sqrt{[Ca^{2+}]/[Na^+]}) \;\; + 2.24} - 273.15 \qquad (8)$$

where [ ] = Concentration of metal ion in moles/kg
β = 1/3 for temperatures > 100°C,
β = 4/3 for temperatures < 100°C

Na-K-Ca-Mg geothermometer. Incorrect high temperatures are indicated by the geothermometer when applied to low-temperature waters relatively rich in Mg (Mg>1 mg/kg) (Nicholson, 1993). The Mg-correction is applied to those geothermal waters that contain high dissolved Mg as the presence of Mg will give anomalously high temperature results if no correction is made.

This correction method is only applicable if T Na-K-Ca >70°C. Fournier and Potter (1979) devised the Mg-correction to the Na-K-Ca geothermometer, using equations with concentrations in mg/kg:

$$R = \frac{C_{Mg}}{C_{Mg} + 0.61C_{Ca} + 0.31C_K} \times 100 \qquad (9)$$

If R > 50, ignore the calculated Na-K-Ca temperature and assume that temperature of the water at depth is approximately the same as the temperature of the water measured in the field.

If R > 5, using the Na-K-Ca temperature in Kelvin, the equation for the Mg-corrected temperature is:

$$\Delta t_{Mg} = 10.664 - 4.7415logR + 325.87(logR)^2 - 1.032 \times 10^5(logR)^2/T_{NaKCa} - 1.968 \times 10^7(logR)^2/T_{NaKCa}^2 + 1.605 \times 10^7(logR)^3/T_{NaKCa}^2 \qquad (10)$$

If R < 5, using the Na-K-Ca temperature in Kelvin, the equation for the Mg-corrected temperature is:

$$\Delta t_{Mg} = -1.03 + 59.971logR + 145.05(logR)^2 - {}^{36711(logR)^2}\Big/_{T_{NaKCa}} \\ - {}^{1.67\times 10^7 logTR}\Big/_{T^2_{NaKCa}} \quad (11)$$

3.3 Mineral-solution equilibrium

Generally, geothermometers are used to estimate the reservoir temperature, but sometimes the geothermometers gives diverse results. Reed and Spycher (1984) have suggested that the best estimate of reservoir temperature can be attained by considering simultaneously the state of equilibrium between the equilibrium states of many hydrothermal minerals in water as a function of temperature.

The equilibrium state of a mineral and solution in a geothermal system can be evaluated by the ratio of the reaction quotient (Q) to the equilibrium constant (K) (Arnórsson, 2000) both of which are related to the Gibbs energy through:

$$\Delta Gr = -RTlnK + RTlnQ = RTln\left(\frac{Q}{K}\right) \quad (12)$$

where R = Gas constant
T = Temperature (K)

The saturation index (SI) for minerals in aqueous solutions at different temperatures can be obtained from:

$$SI = log\left(\frac{Q}{K}\right) = logQ - logK \quad (13)$$

The SI value for each mineral is a measure of the saturation state of the water phase with respect to the mineral phase. Values of SI are SI=0 for equilibrium; SI >0 for a supersaturated solution; SI<0 for an undersaturated solution. If the fluid mixes with dilute water, mineral curves will intersect at SI<0, but if it has boiled they will intersect at SI>0. If the mineral curves intersect at 0 at a particular temperature, that temperature represents the reservoir temperature.

The computer program WATCH (Arnórsson et al., 1982; Bjarnason, 2010) is generally used to calculate the aqueous speciation of geothermal fluids based on chemical analyses of samples collected at the surface. The relationship between the saturation states to temperature for each mineral are shown by log (Q/K) diagrams.

3.4 Mixing

The hot water from a reservoir may be cooled on the way to the surface. Cooling possibly takes place by mixing with shallow cold water. Mixing can affect the geothermometer result which may yield misleading results (Arnórsson, 2000).

It is necessary to recognize whether waters are truly mixed or not before applying mixing models to estimate reservoir temperatures. Linear relationships between the concentrations of conservative components like Cl/B ratio or Cl and δD, or Cl and $\delta^{18}O$, are generally considered to constitute the best evidence for mixing in geothermal systems (Arnórsson, 2000).

Mixing models are an effective method during the early stages of geothermal development. Mixing models can be used to evaluate the heat potential and flow structures of a new geothermal resource, and

also to estimate the hot water component in mixed waters in springs or discharge from shallow drill holes. The three commonly used mixing models are:

1) The chloride-enthalpy mixing model;
2) The silica-enthalpy mixing model;
3) The silica-carbonate mixing model.

The enthalpy-chloride mixing model of Fournier (1979) is very useful for characterizing the parent geothermal liquid, understanding the hydrology of a geothermal field, and to estimate the reservoir temperature. The enthalpy-chloride mixing model has been widely used mainly when the initial temperature of the hot water is above 200°C. High temperature waters (>200°C) are generally relatively rich in carbon dioxide. When cold water mixes with hot water but boiling does not occur, the mixed water becomes acid. The acid waters will dissolve carbon dioxide and are likely to be far from equilibrium with both primary and secondary rock forming minerals and, as a result, they are quite reactive (Arnórsson, 2000).

The silica-enthalpy mixing model of Fournier (1977) is useful to estimate the temperature of the hot water component based on the dissolved silica concentration of a mixed water. In the silica-enthalpy mixing model, the dissolved silica is plotted against the enthalpy of the liquid instead of the temperature due to the combined heat contents of two waters being conserved when these waters are mixed, but the combined temperatures are not. The enthalpy values are obtained from steam tables.

The silica-carbonate mixing model has been proposed by Arnórsson (1985) based on the relationship between dissolved silica and total carbonate concentrations in high temperature systems. This model can be used to distinguish boiled waters from mixed or conductively-cooled discharges, and is useful to estimate the temperature where mixing prevents boiling. The model assumes that all the carbonate is present as CO_2. Due to boiling of the geothermal fluid, the carbon dioxide enters the vapour phase and the residual liquid will be depleted in carbonate (Nicholson, 1993).

4. CHEMICAL CHARACTERISTICS OF THERMAL FLUIDS

Hydrothermal systems have different characteristics according to the region where they're located. These characteristics depend on many factors, like tectonics, temperature, pressure, rock type, permeability, fluid composition, and duration of activity. Geochemistry is one of the methods to investigate relationships between geothermal manifestations and the existence of a subsurface geothermal system. Fluid and gas geochemistry can be used to estimate reservoir conditions, recharge area, and fluid flow. Geothermal fluid composition is controlled by physical and chemical processes. The chemical processes depend on reactions between water and rock, both dissolution and deposition, while physical processes include boiling, cooling, and mixing (Nicholson, 1993).

The chemical composition of hot spring waters can indicate a probable flow which will affect the manifestation type and chemical characteristics. Chemical characteristics can reflect mixing between cold water and hot water from a reservoir. Mixing with cold groundwater will give results showing dilution of geothermal water due to the fact that the solubility of most compounds in the waters will increase with increased temperature.

Seventeen thermal samples from hot springs, warm springs, and cool waters were selected for the present geochemical study. Nine samples were collected by Geological Agency in 2014 and eight samples were collected by Jacobs New Zealand, Ltd. in 2016 during a further investigation. The results of the analysis are shown in Appendix I.

Nicholson (1993) states that the salinity of seawater is fairly constant, at about 35000 mg/L, equivalent to a chloride ion concentration of about 19350 mg/L. In this study, the chloride concentration of several samples is relatively high, more than 10000 mg/kg and a higher salinity than 35000 mg/L (Appendix I). Many are boron-rich and their sulphate concentrations are relatively high. The stable isotope ratios of the thermal water plot are close to the world meteoric line in a $\delta D - \delta^{18}O$ diagram.

4.1 Classification of samples

The Cl-SO_4-HCO_3 ternary diagram is used to classify the geothermal water based on the major anion concentrations, Cl^-, SO_4^{2-}, and HCO_3^-. In the diagram (Figure 5) three major groups of water are shown, mature waters which plot in the top corner and are Cl-rich, peripheral waters which plot in the HCO_3 corner, and volcanic waters with the major anion SO_4^{2-}.

Two thirds the Waesano geothermal waters plot as mature water with about 80% Cl anion concentration. Samples BB-01 and ADCR are cold water samples which plot as peripheral waters. The cold water is CO_2-rich water. The Waesano springs have highly variable sulphate ion concentrations (5 to 1500 ppm) which appear to be generated by the oxidation of H_2S. The presence of SO_4^{2-} in three samples, i.e. WS-06, ADSA, and ADPI indicates that the water possibly comes from volcanic deep water.

The hottest springs in the Waesano geothermal field (WS-02 with a temperature of 97°C) have a very low sulphate concentration and a neutral pH. The spring water with the highest sulphate concentration (WS-06) has the lowest pH which suggests that the acid is from a shallow source generated by the oxidation of H_2S from the spring water. The Waesano water is the alkali chloride type that is typical of a deep geothermal fluid, such as the WS-02, APWS-01, and APWS-02 hot spring waters that have high Cl concentrations and a pH range of about 5 – 6. In general, the geothermal fluids have pH values of about 6 to 7 in the reservoir where water-rock equilibration has prevailed at high temperatures.

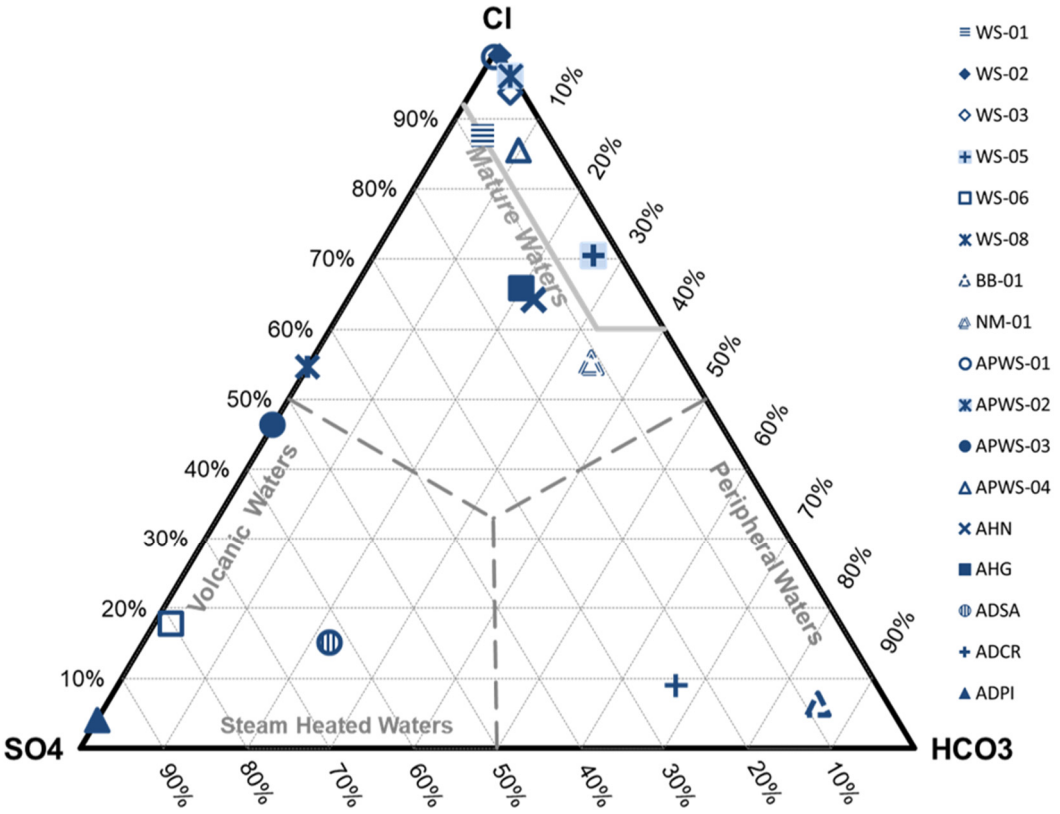

FIGURE 5: Cl-SO_4-HCO_3 ternary diagram for Waesano geothermal waters

4.2 Origin of the geothermal water

The application of stable isotopes in geothermal studies will give information about the origin of water, possibly on underground mixing between different waters, and water-rock interaction. A sample of groundwater discharging from either a cold or a hot spring, with a deuterium value similar to the mean value of the local precipitation, can indicate a local origin of the groundwater (Árnason, 1976).

The oxygen and hydrogen stable isotope ratios ($\delta^{18}O$ and $\delta^{2}H$) are plotted against each other in Figure 6 and show several indications, mostly of cold surface water with a neutral pH such as stream (Appendix I) and waterfall waters (ADCR) plot on the meteoric water line as is characteristic of meteoric water or groundwater. The meteoric water line is the trend along which most cold surface waters plot around the world. Cold water with an acid pH, warm spring waters, and other hot waters plot to the right of the meteoric water line. Most of the hottest spring waters from APWS-01 and WS-02 have a large $\delta^{18}O$ shift of about 5 ‰ to the right of the meteoric water line. Such shifts are normally caused by a high temperature exchange of ^{18}O between water and rock which causes ^{18}O-enrichment.

The Waesano spring waters have a high chloride concentration, close to the seawater concentration of about 19350 mg/L (Nicholson, 1993). Figure 6 shows that APWS-01 water with a high $\delta^{18}O$ but the same δD as the other spring waters displays a horizontal shift which means that the water comes from the same source, but the shift is not due to seawater evaporation but possibly to interaction of the geothermal fluid with the rock. That means that the waters from APWS-01 and WS-02 possibly originate as deep waters but have been diluted by meteoric water to a small extent.

There is one sample WS-08 whose isotope ratios are positive that is the lake water which is highly evaporated as if reflected in its isotope composition which is typical of lake waters and in this case, plots close to seawater. This is coincidental, the lake water has a Cl concentration of 420 ppm only, so it is clearly not seawater.

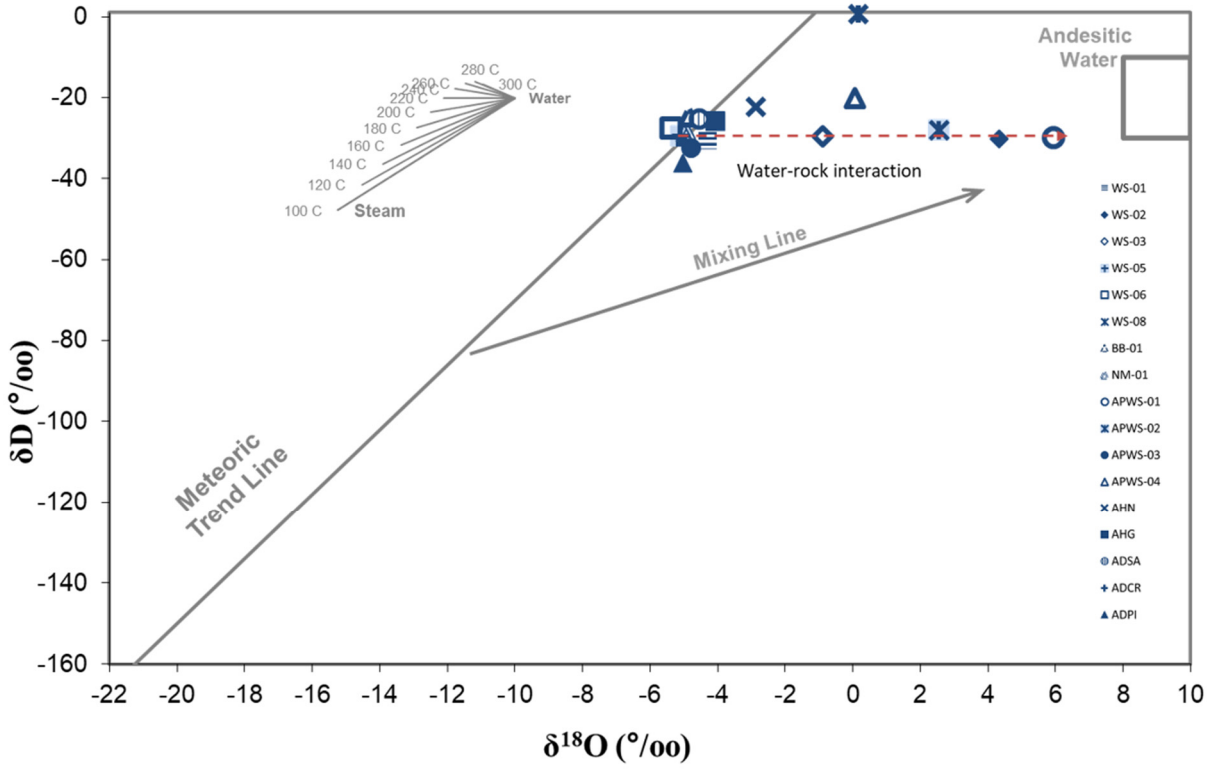

FIGURE 6: Stable isotope ratios in Waesano geothermal waters

The Cl-Li-B ternary diagram can be used to trace the origin of thermal fluids. Figure 7, shows that all samples plot close to the Cl-B line. That is not in agreement with the Cl-SO_4-HCO_3 ternary diagram as almost all Waesano geothermal waters are classified as mature waters. This may indicate that mixing with groundwater takes place when the water moves to the surface.

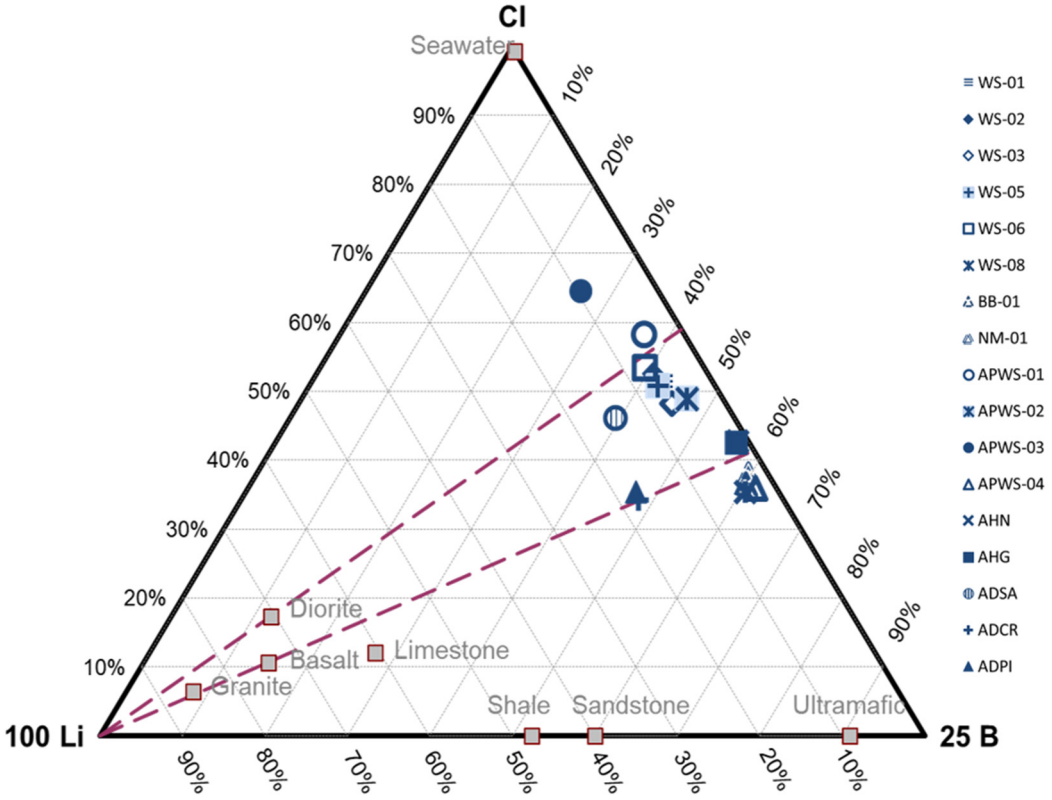

FIGURE 7: Cl-Li-B ternary diagram for Waesano geothermal waters

5. ESTIMATION OF RESERVOIR TEMPERATURE

5.1 The Na-K-Mg ternary diagram

The Na-K-Mg ternary diagram was used for the interpretation of analytical data for hot spring samples. According to Figure 8, only the samples from APWS-01 and WS-02 plot near the full equilibration area. The samples that plot in the partial equilibrium area suggest that interaction of fluid with the rocks in hot conditions has taken place before it mixed with ground water (meteoric water). Both of them give an indication of high temperatures, 225°C for APWS-01 and 265°C for WS-2. The influence of rocks and sediments must be considered in this case, as the Na-K-Mg ternary diagram shows a high temperature but the Na and Cl concentrations are relatively high. The warm spring waters like those from AHG and AHN plot in the partial equilibrium area and suggest a temperature of about 160°C. This temperature is quite low but it gives an indication that there is an influence of rock sediments due to a thick travertine sinter on the surface in the warm springs. Other springs and cold waters like those from ADPI, ADSA, and ADCR plot in the immature waters area.

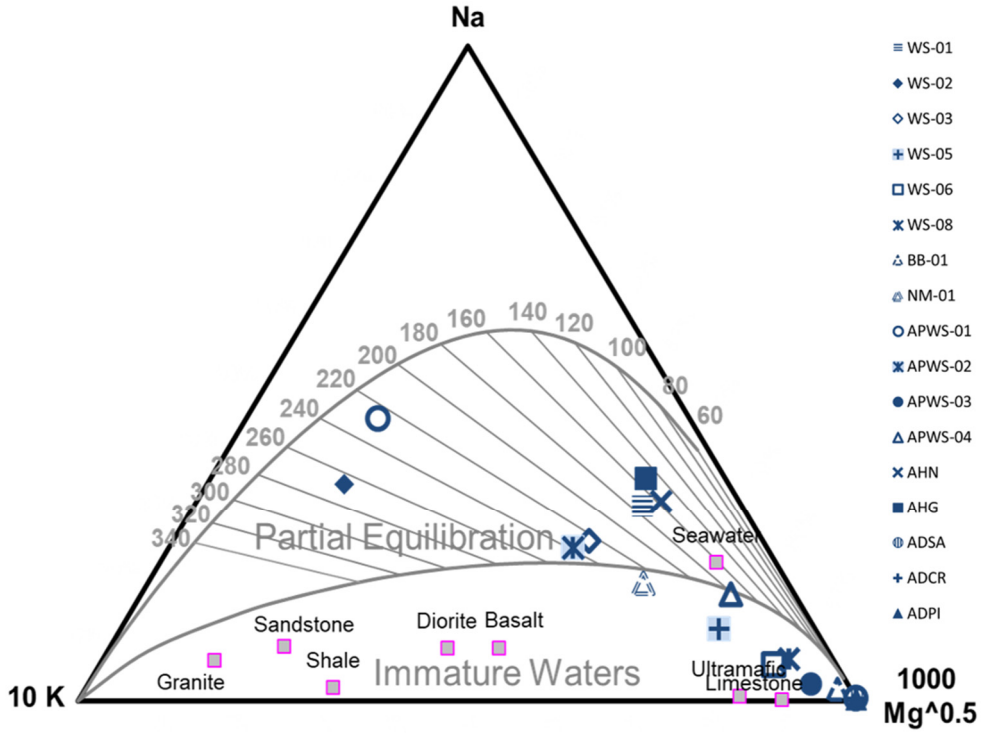

FIGURE 8: Na-K-Mg ternary diagram for Waesano geothermal waters

5.2 Geothermometers

Several geothermometers such as the quartz geothermometer, chalcedony geothermometer, Na-K geothermometer, Na-K-Ca geothermometer, and Na-K-Ca-Mg geothermometer have been used to calculate the subsurface temperature for the Waesano geothermal field. The Na-K-Ca temperature was calculated using the Fournier and Truesdell (1973) equations. The temperatures of the hot springs as determined by geothermometers are shown in Table 3.

Not all the Waesano geothermal samples are suitable for the use of geothermometers. Giggenbach (1991) suggests that the best suited waters for geothermometers are comprised of neutral, low sulphate, high chloride geothermal waters which are close to the Cl corner (mature waters) in the Cl-SO_4-HCO_3 ternary diagram. Of the 17 samples, only seven samples were classified as mature waters and suitable for geothermometry based on the Cl-SO_4-HCO_3 ternary diagram and Na-K-Mg ternary diagram, that is WS-01, WS-02, WS-03, APWS-01, APWS-02, AHN, and AHG. And the other 10 samples such as WS-05, WS-06, WS-08, BB-01, NM-01, APWS-03, APWS-04, ADSA, ADCR, and ADPI are not suitable for geothermometry due to being immature waters (dissolution of rock with little or no chemical equilibrium).

The quartz geothermometer gives the lowest temperature of 106.2°C for APWS-01 and the highest temperature of 167.9°C for WS-03; the chalcedony geothermometer gives the lowest temperature of 76.5°C for APWS-01 and the highest of 158.4°C for WS-03; the Na-K geothermometer gives the lowest temperature of 86.7°C for AHG using the equation from Truesdell (1976) and the highest temperature of 266.2°C for WS-02 using the equation from Giggenbach (1988). The Na-K-Ca geothermometer gives the lowest temperature of 120.1°C for WS-08 and the highest temperature of 277°C for WS-02. It is probably an anomalously high temperature which may be caused by a high concentration of Mg which in most of the samples is quite high (Mg>1 mg/kg, Appendix I) (Nicholson, 1993). It should be checked by the Mg correction for the Na-K-Ca geothermometer, and that correction gives the lowest temperature of 30.2°C for AHN and the highest temperature of 276.4°C for WS-02.

TABLE 3: Temperature estimation from various geothermometers in °C

Sample	T1	T2	T3	T4	T5	T6	T7	T8	T9
WS-01	44.0	152.9	145.8	128.0	229.5	235.4	192.0	209.4	146.7
WS-02	97.0	147.1	141.1	121.6	264.2	266.2	235.2	277.0	276.4
WS-03	55.0	179.6	167.9	158.4	218.7	225.7	179.0	223.3	176.7
WS-05	45.0	153.3	146.2	128.5	235.7	241.0	199.6	176.5	110.8
WS-06	38.0	142.1	136.8	115.9	263.0	265.2	233.7	129.9	110.5
WS-08	27.0	132.0	128.3	104.7	215.3	222.6	174.9	120.1	101.5
BB-01	32.0	163.6	154.8	140.2	226.0	232.3	187.8	79.2	67.9
NM-01	38.0	149.1	142.7	123.8	161.1	173.2	112.2	197.6	92.4
APWS-01	81.6	106.1	106.2	76.5	219.2	226.1	179.5	249.9	249.0
APWS-02	71.1	149.8	143.2	124.5	231.5	237.2	194.5	225.4	184.5
APWS-03	36.8	99.6	100.7	69.6	287.8	287.0	265.7	106.2	92.4
APWS-04	53.9	137.0	132.6	110.3	170.8	182.1	123.1	190.8	60.6
AHN	36.0	108.0	107.9	78.6	143.7	157.0	92.9	194.3	30.2
AHG	36.0	115.9	114.7	87.1	138.1	151.7	86.7	189.6	41.5
ADSA	25.3	41.4	49.2	8.7	-	-	-	-	-
ADCR	23.5	41.4	49.2	8.7	133.3	147.3	81.6	-3.5	75.1
ADPI	25.1	31.7	40.4	1.2	-	-	-	-	-

T1 = Measured temperature; T2 = Quartz geothermometer no steam loss (Fournier, 1977); T3 = Quartz geothermometer with maximum steam loss (Fournier, 1977); T4 = Chalcedony geothermometer (Fournier, 1977); T5 = Na/K geothermometer (Fournier, 1979); T6 = Na/K geothermometer (Giggenbach, 1988); T7 = Na/K geothermometer (Truesdell, 1976); T8 = Na-K-Ca geothermometer (Fournier and Truesdell, 1973); T9 = Na-K-Ca-Mg geothermometer (Fournier and Potter, 1979).

The Na/K geothermometer proved suitable for a high temperature reservoir above 180°C. This geothermometer is applicable to high temperatures due to the re-equilibration being slower than the silica-quartz geothermometer and it is not much affected by mixing. Geothermometers indicate the reservoir temperatures of the Waesano to be 124°C to 252°C based on the average for the Na-K geothermometer.

5.3 Mineral-solution equilibrium

The WATCH 2.4 computer program (Arnórsson et al, 1982, Bjarnason, 2010) was used to calculate the aqueous speciation of geothermal fluids from each hot spring based on results of chemical analysis of the samples with respect to a reservoir temperature that may be arbitrary, measured or obtained by a suitable geothermometer.

The log (Q/K) diagrams (Figure 9) show that no best equilibrium temperatures can be found, possibly due to mixing or boiling or other processes such as the precipitation of some minerals. All waters do not equilibrate with calcite. So, to estimate the reservoir temperature, an intersection from other minerals is used. In WS-01 and APWS-01, anhydrite and quartz seem to reach equilibrium at 125°C. For WS-02 and WS-03, wollastonite and quartz seem to converge at about 200°C, close to the log (Q/K) = 0 line which would suggest a little mixing with cold groundwater. For APWS-02, anhydrite and quartz seem to reach equilibrium at 175°C. For AHN and AHG as warm springs, anhydrite and quartz seem to reach equilibrium at 150°C. That implies that subsurface temperatures of the field are in the range 125°C to 200°C which covers the convergence points on the log (Q/K) diagrams corresponding to the mineral equilibria point. This temperature range is close to the Na/K temperature estimated with an average temperature range of 124°C to 252°C (Table 3).

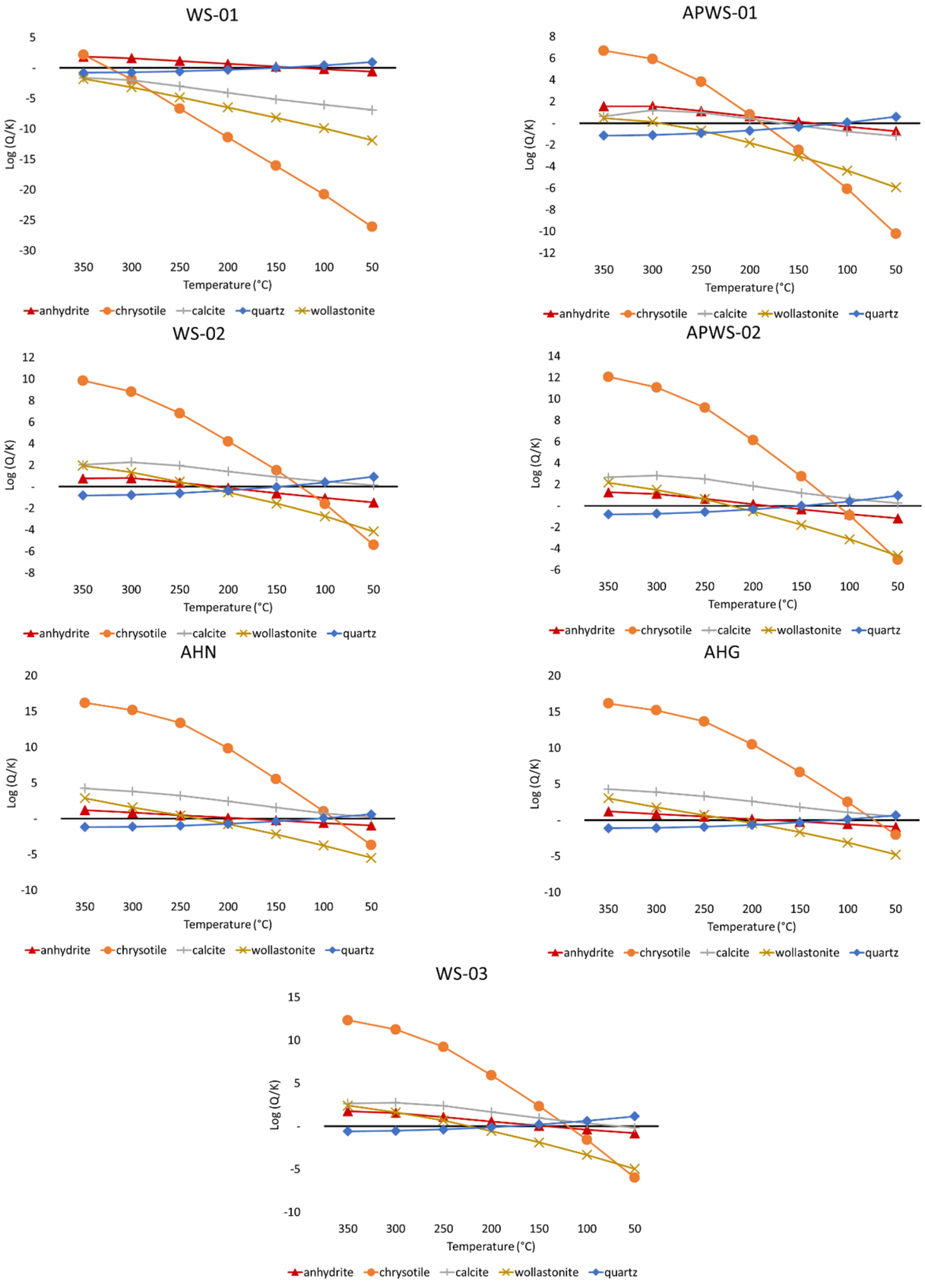

FIGURE 9: Mineral-solution equilibrium diagrams for Waesano geothermal waters

5.4 Mixing models

In general, geothermal water has cooled when it appears at the surface in hot springs. The cooling of reservoir waters takes place when the water is ascending to the surface, by conduction, boiling or mixing with cold water in shallow zones.

Arnórsson (1985) suggests several types of evidence of mixing. The first is the Na-K-Mg ternary diagram (Figure 8). Most samples plot in the partial equilibrium area. The second is the mineral-solution equilibrium diagram (Figure 9). The diagram shows no clear equilibrium between hot water and a group of minerals. The third is linear relationships between Cl and most other constituents observed. In this study, the relationships between Cl and B and the relationship between Cl and $\delta^{18}O$ were studied. Figures 10 and 11 show evidence of a linear relationship between Cl and B concentrations and a linear relationship between Cl and $\delta^{18}O$, suggesting that the ascending water might have mixed with cold groundwater in the upflow zones. There are several signs that the Waesano geothermal water has possibly mixed with cold water.

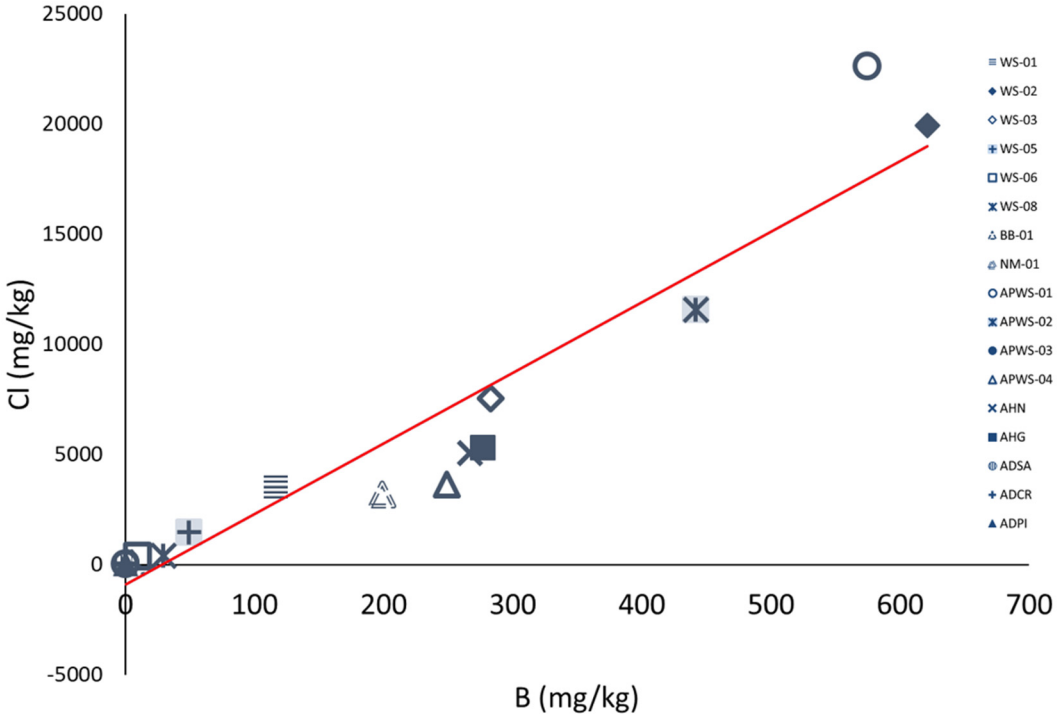

FIGURE 10: Cl/B ratio for Waesano geothermal waters

Silica-enthalpy mixing model. A silica-enthalpy mixing model was suggested by Truesdell and Fournier (1977) to estimate the temperature of the hot water component in a mixed water. Enthalpy values used to estimate the Waesano reservoir temperatures were derived from measured spring temperatures and steam tables (Keenan et al., 1969), and samples ADSA, ADCR, and ADPI were used as the reference cold water.

Figure 12 shows the silica-enthalpy mixing model applied to the Waesano geothermal system. In this model, the cold water samples are from ADSA, ADCR, and ADPI. Four mixing lines have been plotted. The intersection of cold water and spring water with the quartz solubility curve gives results for temperature estimation on line-a and line-b, which indicate the composition of the parent geothermal water prior to mixing. Mixing line-a connects a cold water sample to hot water sample APWS-01 and intersects the quartz solubility curve at an the enthalpy value of about 590 kJ/kh, which corresponds to an original temperature of 140°C for the hot water component. Mixing line-b, connects a cold water sample to hot water sample WS-02 and intersects the quartz solubility curve at an enthalpy value of

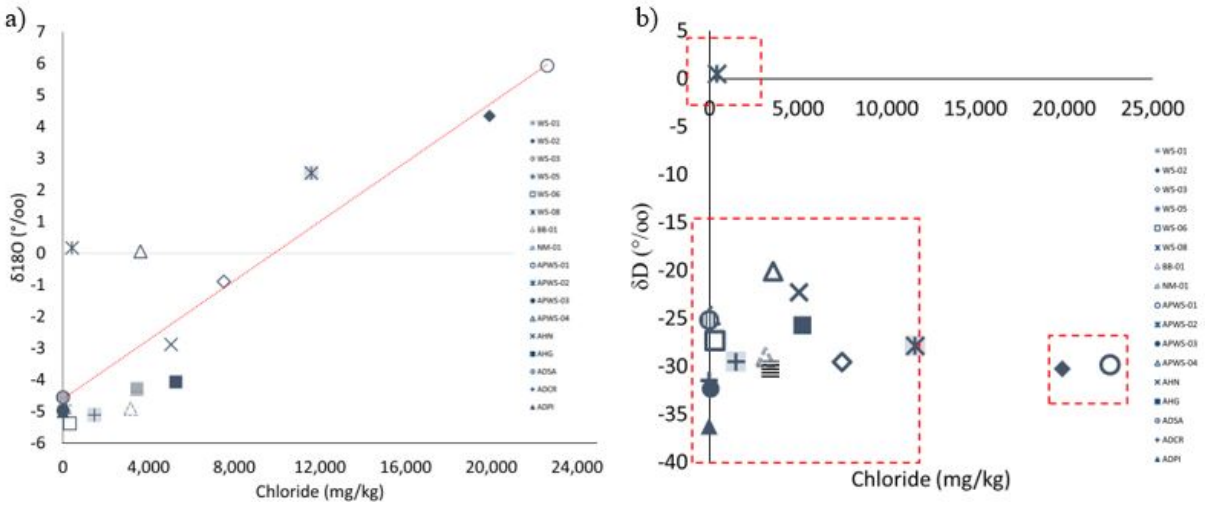

FIGURE 11: The relationship between Cl and a) $\delta^{18}O$ (‰) and b) δD (‰) for Waesano geothermal waters

about 910 kJ/kg, which corresponds to an original temperature of 213°C for the hot water component. Results obtained by the silica-enthalpy model were slightly higher than those estimated by silica geothermometers and ranged on average between 77 and 173°C. These results show that temperature may be underestimated due to silica precipitation caused by mixing with cold water and cooling.

The relationship between the cold water and the thermal waters, assuming separation and steam escape (100°C, 419 kJ/kg), is described by lines-c and -d in in Figure 12. Thus, the reservoir temperature is evaluated by connecting horizontal lines to the quartz solubility curve corresponding to the maximum

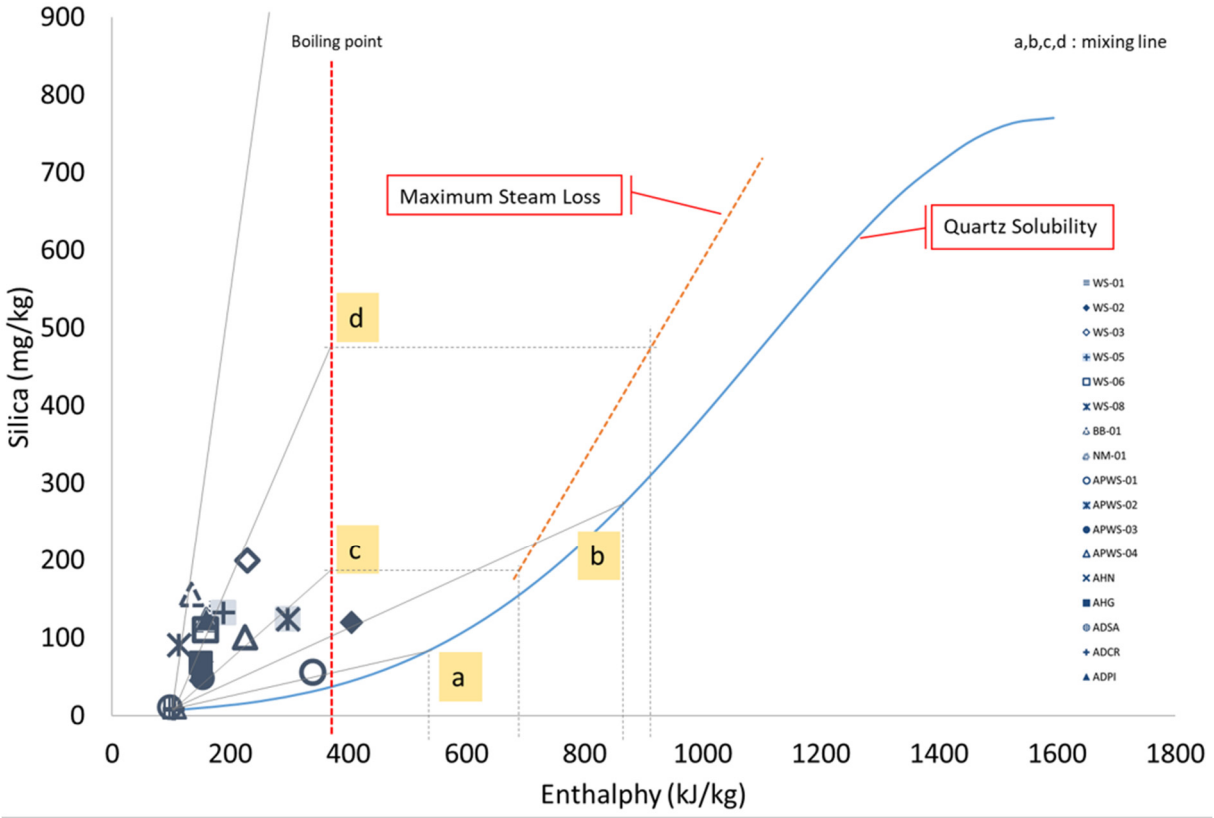

FIGURE 12: Silica-enthalpy mixing model for Waesano geothermal waters (Truesdell and Fournier, 1977)

boiling line, while a vertical line will intersect the quartz solubility no steam loss curve and gives the indication of the original silica concentration and temperature in the reservoir. Mixing line-c connects cold water samples to hot water samples APWS-03, APWS-04, and APWS-02, and intersects the boiling line and gives an enthalpy value of about 720 kJ/kg, which corresponds to an original temperature of 170°C for the hot water component. Mixing line-d connects a cold water sample to hot water sample AHG, WS-06, WS-05, and WS-03, and intersects the boiling line and gives an enthalpy value of about 980 kJ/kg, which corresponds to an original temperature of 228°C for the hot water component. The silica concentrations of samples WS-08 and BB-01 are higher, probably due to boiling.

Enthalpy-chloride mixing model. Fournier (1979) suggested an enthalpy-chloride diagram to characterize the parent geothermal water and to predict reservoir temperature. The enthalpy-chloride mixing model for Waesano geothermal waters is shown in Figure 13. The model shows that the spring waters possibly originate in a different hydrothermal system. Line-a connects the cold groundwater samples to samples APWS-03, WS-06, and BB-01. Line-b connects the cold water samples to sample WS-05. Line-c connects the cold water samples to samples NM-01, WS-01, and APWS-04. Line-d connects the cold water samples to warm spring samples AHN, AHG, and WS-03. Line-e connects the cold water samples to WS-08, and line-f connects the cold water samples to WS-02. The models indicate the lowest temperature of 143°C from sample WS-02, which is a similar temperature to the quartz geothermometer temperature and is probably close to the reservoir temperature.

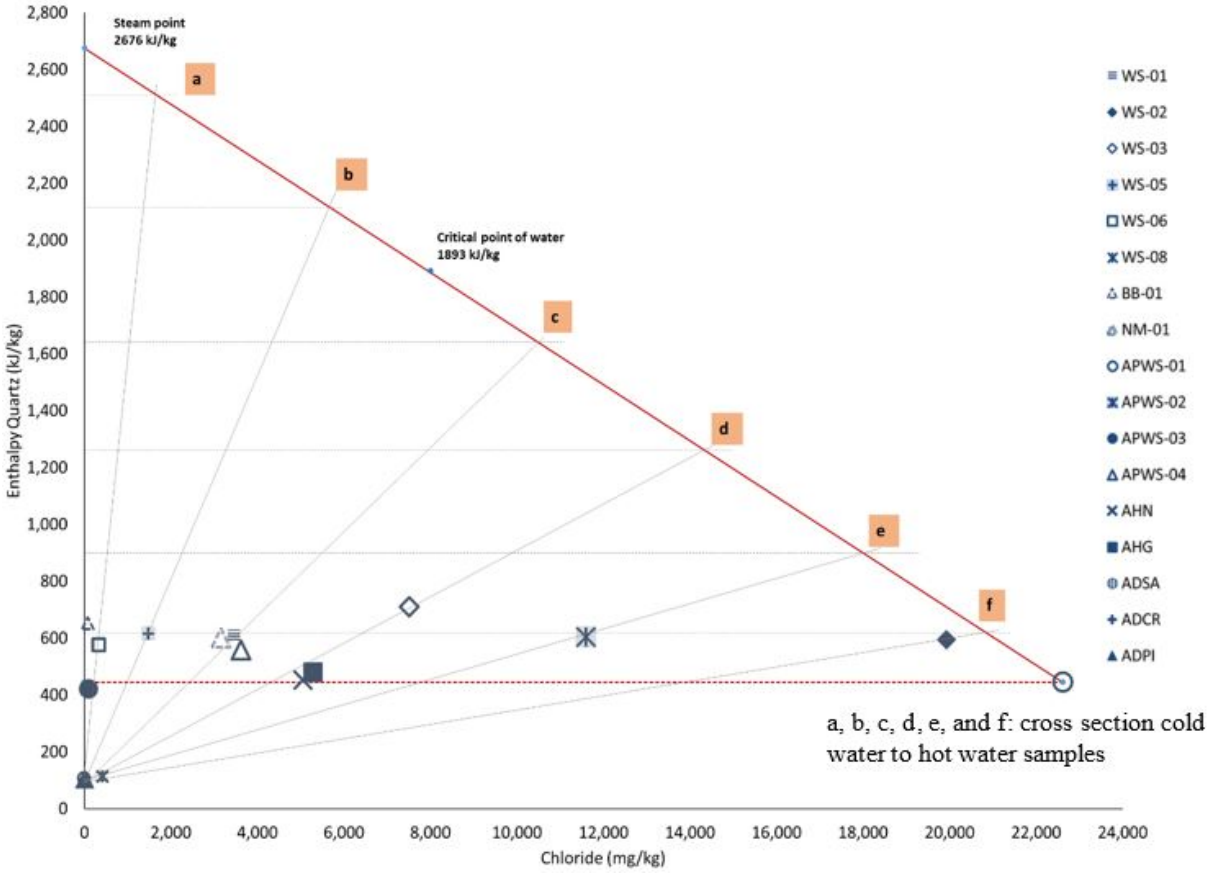

FIGURE 13: Enthalpy-chloride mixing model for Waesano geothermal waters

The two mixing models suggest that the APWS-01 and WS-02 waters are deep waters, possibly mixed with a small amount of meteoric water. This result is consistent with the stable isotope results (Figure 6).

6. CONCLUSIONS

The purpose of this report is to study how to determine the type and origin and to estimate the subsurface temperature of the hot springs/warm springs from the Waesano geothermal area using their chemical composition. The conclusions of this study are as follows:

1. The Cl-SO_4-HCO_3 and Na-K-Mg ternary diagrams characterise the waters from the Waesano geothermal area as chloride rich, plotting close to the area of mature geothermal fluids and in the partially equilibrated area. The type of hot spring /warm spring water in the Waesano geothermal area is chloride-sulphate.

2. The Waesano geothermal system is a volcanic geothermal system influenced by sedimentary rocks. The hottest springs in Waesano (APWS-01 and WS-02, 97°C) show the presence of a deep reservoir with water with a near-neutral pH, saline, and rich in chloride and boron.

3. Temperature estimation by various geothermometers gives the reservoir temperature range between 124 and 252°C based on the Na/K geothermometer. Temperature estimates by the Na-K geothermometer mostly yield temperatures higher than those obtained by silica geothermometers. In this study, the Na-K temperature is probably most suitable for the Waesano geothermal system due to its slow re-equilibrium after cooling and because it is less affected by mixing with cool groundwater. The temperature obtained from log (Q/K) diagrams is in the range of 125-200°C, close to the Na-K average temperature, which is then interpreted as the reservoir temperature. Two types of mixing models have been applied to evaluate the temperature of the hot water component in the geothermal reservoir, the chloride-enthalpy model and the silica-enthalpy model. Together they indicate a subsurface temperature in the range of 140-213°C.

4. Based on several methods that have been used to estimate the reservoir temperature, the Waesano geothermal field is a medium temperature system with a temperature range of 200±70°C.

5. The analytical results for $\delta^{18}O$ and δD show that cold groundwater and warm spring water plot close to the meteoric water line, while the hot water may be directly derived from deep water with the possibility of dilution by a small amount of meteoric water. The samples from the hottest springs in Waesano (APWS-01 and WS-02, 97°C) plot with a large $\delta^{18}O$ isotope shift of about 5 ‰ from the meteoric water line. The origin of the unusually high salinity in APWS-01 and WS-02 is not condensation of sea water, as the δD has not increased at the same time as the $\delta^{18}O$ has shifted. It is possible that the origin of this water is deep water followed by water-rock interaction. The water-rock interaction has possibly taken place in a sedimentary formation considering the salinity of the sample.

ACKNOWLEDGEMENTS

I would like to thank the United Nations University Geothermal Training Programme (UNU-GTP) for granting me this opportunity to participate in the 6-month training programme in Iceland. Special thanks go to Mr. Lúdvík S. Georgsson and staff members of UNU-GTP, Mr. Ingimar G. Haraldsson, Mr. Markús Andri Gordon Wilde, Ms. Málfrídur Ómarsdóttir, and Ms. Thórhildur Ísberg for their assistance and arrangement in the past six months during the training programme and my stay in Iceland.

My sincere gratitude and acknowledgement to Dr. Halldór Ármannsson, my advisor, for his experience and knowledge of geochemistry, valuable advice and assistance during the writing of the report. The highest appreciation and gratitude go to all the lecturers for a variety of valuable lessons and willingness to share their knowledge and experience, especially in geochemistry. I also feel grateful and thankful to my geochemistry fellows, Eunice Anyango Bonyo from Kenya, Syed Hilal Farooq from India, and

Yerko Figueroa Penarrieta from Bolivia, for laughs, discussions and suggestions during the training period. And of course, many thanks to my Indonesian fellows, Gloria Gladis Sondakh and Adhiguna Satya Nugraha who always take care of each other.

Finally, many thankful acknowledgements to the Directorate of Geothermal, Ministry of Energy and Mineral Resources of Republic of Indonesia for their help, support and allowing me to attend the 6-month training programme at the UNU-GTP. And my deepest thanks go to my family for their support and encouragement during the period of the training programme.

To the 2018 UNU Fellows, thank you for your cheer and friendship in the whole six months. Hope to see you again in the future.

REFERENCES

Árnason, B., 1976: *Groundwater systems in Iceland traced by deuterium*. Soc. Sci. Islandica, 42, Reykjavík, 236 pp.

Arnórsson, S., 1985: The use of mixing models and chemical geothermometers for estimating underground temperature in geothermal systems. *J. Volc. Geotherm. Res., 23*, 299-335.

Arnórsson, S. (ed.), 2000: *Isotopic and chemical techniques in geothermal exploration, development and use. Sampling methods, data handling, interpretation*. International Atomic Energy Agency, Vienna, 351pp.

Arnórsson, S., Andrésdóttir, A., Gunnarsson, I., and Stefánsson, A., 1998: New calibration for the quartz and Na/K geothermometers - valid in the range 0-350°C (in Icelandic), *Proceedings of the Geoscience Society of Iceland Annual Meeting, April*, 42-43.

Arnórsson, S., Gunnlaugsson, E., and Svavarsson, H., 1983: The chemistry of geothermal waters in Iceland. III. Chemical geothermometry in geothermal investigations. *Geochim. Cosmochim. Acta, 47*, 567-577.

Arnórsson, S., Sigurdsson, S., and Svavarsson, H., 1982: The chemistry of geothermal waters in Iceland I. Calculation of aqueous speciation from 0°C to 370°C. *Geochim. Cosmochim. Acta, 46*, 1513-1532.

Barber, P., Carter, P., Fraser, T., Baillie, P., and Myers, K., 2003: Paleozoic and Mesozoic petroleum systems in the Timor and Arafuru seas, Eastern Indonesia. *Proceedings, Indonesia Petroleum Association, IPA 29th Annual Convention & Exhibition*, 16 pp.

Bjarnason, J.Ö. 2010: *The speciation program WATCH. Version 2.4, user's guide*. The Icelandic Water Chemistry Group, Reykjavík, 9 pp.

Craig, H., 1963: The isotopic geochemistry of water and carbon in geothermal areas. In: Tongiorgi, E. (ed.), *Nuclear geology on geothermal areas*. Consiglio Nazionale delle Ricerche, Laboratorio di Geologia Nucleare, Pisa, 17-53.

Directorate of Geothermal, 2017: *Geothermal potential of Indonesia Part 2*, Ministry of Energy and Mineral Resources (in Bahasa).

Fournier, R.O., 1973: Silica in thermal waters. Laboratory and field investigations. *Proceedings of the International Symposium on Hydrogeochemictry and Biochemistry, Tokyo, 1, Clark Co., Washington D.C.*, 122-139.

Fournier, R.O., 1977: Chemical geothermometers and mixing models for geothermal systems. *Geothermics, 5*, 41-50.

Fournier, R.O., 1979: A revised equation for Na-K geothermometer. *Geoth. Res. Council, Trans., 3,* 221-224.

Fournier, R.O., and Potter, R.W. II, 1979: Magnesium correction to the Na-K-Ca geothermometer. *Geochim. Cosmochim. Acta, 43,* 1543-1550.

Fournier, R.O., and Potter, R.W., 1982: An equation correlating the solubility of quartz in water from 25° to 900°C at pressures up to 10,000 bars. *Geochim*. *Cosmochim Acta, 46*, 1969-1973.

Fournier, R.O., and Truesdell, A.H., 1973: An empirical Na-K-Ca geothermometer for natural waters. *Geochim. Cosmochim. Acta*, *37*, 1255-1275.

Giggenbach, W.F., 1988: Geothermal solute equilibria. Derivation of Na-K-Mg-Ca geoindicators. *Geochim. Cosmochim. Acta, 52*, 2749-2765.

Giggenbach, W.F., 1991: Chemical techniques in geothermal exploration. In: D'Amore, F. (coordinator), *Application of geochemistry in geothermal reservoir development*. UNITAR/UNDP publication, Rome, 119-144.

Gíslason, S.R., Heaney, P.J., Oelkers, E.H., and Schott, J., 1997: Kinetic and thermodynamic properties of moganite, a novel silica polymorph. *Geochim. Cosmochim. Acta, 61*, 1193-1204.

Hadi, M.N., Kusnadi, D., and Simarmata, R.S.L., 2003: *Geology and geochemistry survey in Waesano, district West Manggarai, East Nusa Tenggara.* Geological Agency of Indonesia (in Indonesian), unpublished report.

Johnstone, R.D., 2005: Contrasting geothermal fields along the magmatic banda arc, Nusa Tenggara, Indonesia, *Proceedings of the World Geothermal Congress 2005, Antalya, Turkey*, 8 pp.

Keenan, J.H., Keyes, F.G., Hill, P.G., and Moore, J.G., 1969: *Steam tables (International edition - metric units).* John Wiley, N.Y. 162 pp.

Mainza, D., 2006: The chemistry of geothermal waters of SW-Uganda. Report 12 in: *Geothermal training in Iceland 2006.* UNU-GTP, Iceland, 219-244.

Nasution, A., Muraoka, H., Rani, M., Takashima, I., Takahashi, M., Akasako, H., Matsuda, K., and Badrudin, M., 2002: Geothermal prospects of Flores Island in Indonesia viewed from their volcanism and hot water geochemistry. *Bull. Geol. Surv. Japan, 53-2/3*, 87-97.

Nicholson, K., 1993: *Geothermal fluids: chemistry and exploration techniques*. Springer-Verlag, Berlin, 268 pp.

Reed, M.H., and Spycher, N.F., 1984: Calculation of pH and mineral equilibria in hydrothermal water with application to geothermometry and studies of boiling and dilution. *Geochim. Cosmochim. Acta, 48*, 1479-1490.

Truesdell, A.H., 1976: Summary of section III – geochemical techniques in exploration. *Proceedings of the 2nd U.N. Symposium on the Development and Use of Geothermal Resources, San Francisco, 1*, 1iii-1xxix.

Truesdell, A.H., and Fournier, R.O., 1977: Procedure for estimating the temperature of a hot water component in a mixed water using a plot of dissolved silica vs. enthalpy. *U.S. Geol. Survey J. Res., 5,* 49-52.

APPENDIX I: Results of analysis of chemical samples used

Location	Description	Code	Elev.	Temp.	pH	Li	Na	K	Ca	Mg	Al	Fe	Cl	F	SO_4	HCO_3	B	SiO_2	NH_3	As	TDS
			m	°C		mg/kg															
Waesano	Hot spring	WS-01	673	44.0	2.9	4.30	1712.0	178.0	429.0	37.0		7.90	3467.0	<0.08	312.0	183.0	117.0	131.0			6580
Waesano	Hot spring	WS-02	671	97.0	6.4	25.00	9111.0	1357.0	2285.0	24.0		0.29	19921.0	0.25	29.0	153.0	621.0	119.0	6.1		33710
Waesano	Hot spring	WS-03	670	55.0	6.1	10.10	3576.0	329.0	1119.0	62.0		0.33	7505.0	<0.03	127.0	374.0	283.0	199.0			13580
Waesano	Hot spring	WS-05	672	45.0	5.9	2.00	719.0	80.0	198.0	25.0		0.22	1473.0	0.04	67.0	553.0	49.0	132.0			3300
Waesano	Hot spring	WS-06	670	38.0	1.7	0.45	163.0	24.0	67.0	6.8		46.00	337.0	0.05	1525.0	40.0	10.0	109.0			2330
Waesano	Lake outflow	WS-08	670	27.0	2.6	0.48	215.0	19.0	77.0	9.0		11.00	421.0	0.05	351.0	<20.0	29.0	91.0			1240
Bobok	Warm spring	BB-01	315	32.0	5.9	0.07	90.0	9.0	87.0	24.0		28.00	76.0	0.04	101.0	1030.0	5.0	156.0			1610
Nampar Macing	Warm spring	NM-01	140	38.0	7.7	2.00	2938.0	127.0	153.0	33.0		1.00	3159.0	1.50	640.0	1923.0	199.0	123.0			9300
Waesano	Hot spring	APWS-01	647	81.6	5.8	18.88	12174.0	1125.9	1990.5	23.4	0.04	0.56	22615.0	0.00	197.0	74.7	574.9	54.7	35.0	1.80	35644
Waesano	Hot spring	APWS-02	646	71.1	6.2	10.24	4371.7	464.5	1979.3	94.1	0.03	0.38	11590.2	0.00	46.0	414.6	441.5	124.4	10.4	0.20	24120
Waesano	Hot spring	APWS-03	680	36.8	3.7	0.13	44.9	8.3	17.3	2.8	0.09	0.66	89.6	0.00	104.1	0.0	1.5	47.7	0.5	0.00	420
Waesano	Hot spring	APWS-04	646	53.9	5.9	2.59	1997.0	99.3	309.7	87.0	0.01	3.55	3616.2	0.00	199.6	412.1	249.1	99.7	9.0	0.50	7504
Nampar Macing	Warm spring	AHN	159	36.0	6.8	1.77	4126.0	136.1	83.7	65.7	0.01	0.87	5047.9	0.00	1060.7	1741.0	267.4	56.9	4.9	0.20	11356
Golo Lara	Warm spring	AHG	111	36.0	7.1	1.56	4358.0	131.2	87.9	52.1	0.05	1.17	5281.1	0.00	1133.6	1621.0	277.3	66.9	6.9	0.50	12053
Sapo	Cold water	ADSA	606	25.3	7.7	0.01	3.6	0.0	2.6	1.7	0.02	0.27	3.2	0.04	13.3	4.8	0.1	10.7	0.2	0.00	40
Cunca Rami	Cold water	ADCR	405	23.5	7.9	0.01	2.9	0.1	1.8	1.4	0.03	0.12	1.9	0.03	5.2	14.4	0.1	10.7	1.0	0.00	35
Pinggong	Cold water	ADPI	389	25.1	4.5	0.01	3.4	0.0	14.4	1.9	0.09	0.16	2.1	0.07	49.3	0.0	0.1	7.9	0.3	0.00	72